Adsorption of finite polymers in different thermodynamic ensembles

Monika Möddel [a,*], Wolfhard Janke [a], Michael Bachmann [b]

[a] *Institut für Theoretische Physik and Centre for Theoretical Sciences (NTZ), Universität Leipzig, Postfach 100 920, D-04009 Leipzig, Germany*
[b] *Institut für Festkörperforschung, Theorie II, Forschungszentrum Jülich, D-52425 Jülich, Germany*

A B S T R A C T

We investigate the cooperative effects of a single finite chain of monomers near an attractive substrate by first constructing a conformational pseudo-phase diagram based on the thermal fluctuations of energetic and structural quantities. Then, the adsorption transition is analyzed in more detail. This is conveniently done by a microcanonical analysis of densities of states obtained by extensive multicanonical Monte Carlo simulations. For short chains and strong surface attraction, the microcanonical entropy turns out to be a convex function of energy in the transition regime. This is a characteristic physical effect and deserves a careful consideration in analyses of cooperative macrostate transitions in finite systems.

© 2010 Elsevier B.V. All rights reserved.

1. Introduction

The understanding of the adsorption phenomena of polymers on surfaces is a prerequisite, e.g., for designing micro- or nanostructures. Also the fact that various polymers are usually found near both sides of cell membranes and are important for their mechanical stability and physiological function [1] has driven studies of polymers near surfaces and interfaces [2]. In this context a deeper understanding of the origin of specific binding affinities of proteins regarding the type of the substrate and the amino acid sequence is very desirable. In recent years, some progress has been made in this field [3,4], but due to the complexity introduced by the huge amount of possible sequences and surfaces many problems are still open. A qualitative understanding of the cooperative nature of the adsorption transition for short chains can, however, already be gained by studying the behavior of homopolymers close to a flat substrate [5–7]. We focus here on the systematic description of the phase diagram in a wide parameter range and cooperative effects of chains of finite length.

First, in this numerical study, the conformational pseudo-phase diagram of a coarse-grained non-grafted off-lattice polymer will be constructed versus temperature and surface attraction strength. The competition between monomer–monomer and surface–monomer attraction gives rise to a variety of different conformational phases [8,9]. Our computer simulations rely on the multicanonical Monte Carlo method [10] that allows for the precise determination

of the canonical expectation values of suitable observables over a wide range of temperatures within a single long simulation run. In addition it yields an estimate of the density of states, which possesses a convex regime at the adsorption transition in the case of short chains and strong surface attraction. Albeit known to be a continuous transition in the thermodynamic limit of infinitely long chains [5], the adsorption transition of non-grafted finite-length polymers thus exhibits a clear signature of a first-order-like transition, with coexisting phases of adsorbed and desorbed conformations.

2. Model and simulation

2.1. Off-lattice homopolymer with attractive substrate

We employ a coarse-grained off-lattice model for homopolymers that has also been generalized for studies of heteropolymers [11] and helped to understand protein folding channels from a mesoscopic perspective [12]. Adjacent monomers are connected by rigid bonds of unity length, but bond and torsional angles are free to rotate. The energy function consists of three terms,

$$E = 4 \sum_{i=1}^{N-2} \sum_{j=i+2}^{N} \left(r_{ij}^{-12} - r_{ij}^{-6} \right) + \frac{1}{4} \sum_{i=1}^{N-2} \left[1 - \cos(\vartheta_i) \right]$$
$$+ \epsilon_s \sum_{i=1}^{N} \left(\frac{2}{15} z_i^{-9} - z_i^{-3} \right), \tag{1}$$

where the first two terms give the energy of a polymer in bulk (E_{bulk}) that consists of the standard 12-6 Lennard–Jones (LJ) potential and a weak bending energy. The bending energy pro-

* Corresponding author.
E-mail addresses: Monika.Moeddel@itp.uni-leipzig.de (M. Möddel), Wolfhard.Janke@itp.uni-leipzig.de (W. Janke), m.bachmann@fz-juelich.de (M. Bachmann).

vides a penalty for successive bonds deviating from a straight arrangement. Here $0 \leqslant \vartheta_i \leqslant \pi$ denotes the bending angle between monomers i, $i+1$, and $i+2$. The distance between the monomers i and j is r_{ij} and z_i is the distance of the ith monomer to the substrate. The third term is the attractive surface potential E_{surf}, obtained by integrating over the continuous half-space $z < 0$, where every space element interacts with a single monomer by the usual 12-6 LJ expression [13]. Hence, the parameter ϵ_s weighs the monomer–surface (E_{surf}) and monomer–monomer (E_{bulk}) interaction. Center-of-mass translation is restricted by the attractive substrate at $z = 0$ and a sufficiently distant steric wall at $z = L_z$. In our microcanonical analysis it will become clear how L_z influences the results, however, the effect on the canonical data is small if L_z exceeds the extension of the polymer. As long as not mentioned otherwise, the ratio N/L_z is kept constant ($L_z = 3N$). We always employ natural units ($k_B \equiv 1$).

2.2. Energetic and structural quantities

To describe the canonical equilibrium behavior, we use the canonical expectation values and thermal fluctuations of the following quantities: energy and specific heat, c_V, the radius of gyration, $\langle R_{gyr} \rangle$, as a measure for the extension of the polymer, and its tensor components parallel and perpendicular to the surface, $\langle R_\parallel \rangle$ and $\langle R_\perp \rangle$, with $R_{gyr}^2 = R_\parallel^2 + R_\perp^2$. The components are of interest due to the structural anisotropy introduced by the substrate. Other useful quantities are the distance of the center-of-mass of the polymer to the surface, $\langle z_{cm} \rangle$, and the mean number of monomers docked to the surface.

2.3. Multicanonical sampling

The density of states $g(E)$ encodes all information regarding the phase behavior of the system rendering its precise estimation extremely helpful. This requires the application of sophisticated Monte Carlo methods. In this work, we have performed multicanonical simulations [10]. The idea is to increase the sampling rate of conformations being little favored in the free-energy landscape by performing a random walk in energy space. This is achieved by introducing suitable multicanonical weights $W_{muca}(E) \sim g^{-1}(E)$ to sample conformations $\mathbf{X}$ according to a transition probability

$$\omega(\mathbf{X} \to \mathbf{X}') = \min\left[W_{muca}(E(\mathbf{X}'))/W_{muca}(E(\mathbf{X})), 1 \right]. \quad (2)$$

As the weights $W_{muca}(E)$, i.e. $g(E)$, are unknown a priori, they are determined iteratively until the energy histogram is constant up to a variation of about 10% in the desired energy range. An efficient, error-weighted multicanonical recursion is described in Ref. [14].

3. Pseudo-phase diagram

To construct the conformational pseudo-phase diagram, multicanonical simulations [10] for 51 different surface attraction strengths $\epsilon_s \in [0, 5]$ were performed for a chain with $N = 20$ monomers. These data can now be reweighted to arbitrary temperature, but since it turns out that the interval $T \in (0, 3]$ is the most interesting one, we restrict ourselves to this range here. Each simulation consisted of 10^8 sweeps and was performed with at least two different initializations. The final pseudo-phase diagram is shown in Fig. 1 and representative conformations are given in Fig. 2. The blue (in the web version) bands indicate the approximate phase boundaries that have some uncertainty because the peaks of the fluctuations of canonical expectation values do not coincide for finite systems. It should be stressed that due to the finite chain lengths all phases and transitions here are not phases in
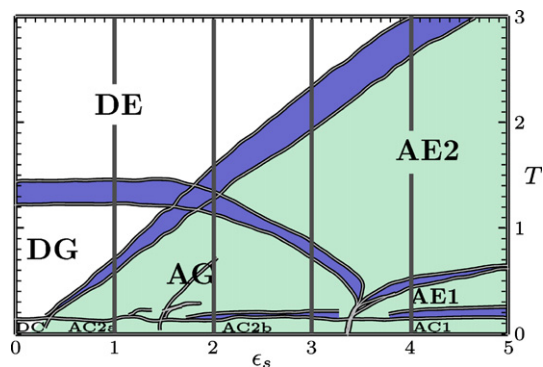

Fig. 1. Pseudo-phase diagram of the 20mer (for details, see text). Different representative conformations are shown in Fig. 2. Along the lines of constant ϵ_s a microcanonical analysis has been performed, see Section 4.

Fig. 2. Representative examples of conformations for the 20mer in the different regions of the T-ϵ_s pseudo-phase diagram in Fig. 1. DE, DG, and DC represent desorbed "phases". In regions AE1, AE2, AC1, AG, AC2a, and AC2b, conformations are favorably adsorbed.

the strict thermodynamic sense. Nevertheless, a reasonable picture of polymer adsorption behavior is obtained and most of the phases are believed to still exist for longer chains. Here, only some representative observables used for the construction will be discussed. For more details, see Ref. [9].

3.1. Energetic fluctuations

Although the energy varies smoothly with T and ϵ_s, two transitions can be identified as ridges in the profile of the specific heat: The *adsorption transition* separating desorbed and adsorbed conformations and a *freezing transition* at low temperatures. Near $T = 0.25$, c_V exhibits a pronounced peak independently of ϵ_s. The crystalline shape of the structures below this peak additionally confirms its nature as freezing transition. However, to identify different crystalline shapes, a closer look at the conformational quantities is needed.

3.2. Structural fluctuations

The average radius of gyration $\langle R_{gyr} \rangle$ reveals that the most compact conformations dominate at low T and low ϵ_s. It establishes the phase boundaries between DE (desorbed expanded) and
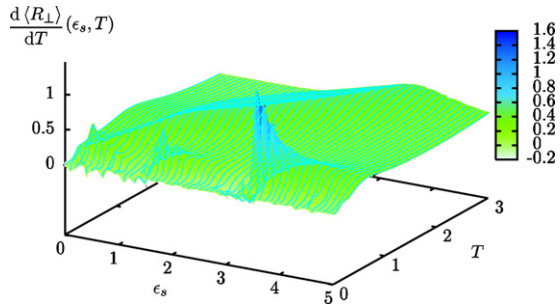
Fig. 3. $\mathrm{d}\langle R_\perp \rangle / \mathrm{d}T$ of the 20mer.

DG (desorbed globular) and between AE2 (adsorbed extended; not flat on substrate) and AG (adsorbed globular) and confirms the freezing transition, but the adsorption transition is not prominently signaled by $\langle R_{\mathrm{gyr}} \rangle$. Its tensor components give additional information. For example, for $\epsilon_s \geqslant 3.4$, $\langle R_\perp \rangle$ vanishes at low T, whereas $\langle R_\parallel \rangle$ attains low values at lower ϵ_s. Small values of $\langle R_\perp \rangle$ correspond to conformations spread out flat on the surface, with associated pseudo-phases AC1 (adsorbed compact; flat) and AE1 (adsorbed expanded; flat), separated by the freezing transition. The most pronounced transition is the strong layering transition at $\epsilon_s \approx 3.4$ that separates regions of planar conformations (AC1, AE1) from the region of double-layer structures (AC2b) and adsorbed globules (AG), below and above the freezing transition, respectively. This sharp energetic transition can, e.g., be nicely seen in $\mathrm{d}\langle R_\perp \rangle / \mathrm{d}T$ in Fig. 3. Although for the considered short chains no higher-layer structures are observed, $\langle R_{\parallel,\perp} \rangle$ indicate some activity for lower ϵ_s. For $N = 20$, $\epsilon_s \approx 1.4$ is the lowest attraction strength, where stable double-layer conformations are found. What follows is a low-temperature subphase of surface attached compact conformations (AC2a). These structures occur if the surface attraction is not strong enough to induce the formation of compact layers. Structures here are subject to quite strong finite-size effects. Raising the temperature above the freezing transition starting in the AC2 regions, polymers adopt the adsorbed, globular, but unstructured conformations of the AG phase. This pseudo-phase has been first conjectured from short exact enumeration studies of 2D polymers in poor solvent [15], but was also found in lattice-polymer simulation studies [6,8]. At even higher T, two scenarios can be distinguished depending on the relative strengths of E_{bulk} and E_{surf}. For low ϵ_s, the polymer first desorbs (from AG to DG) and expands at even higher temperatures (from DG to DE). For larger ϵ_s, the polymer expands while it is still adsorbed (from AG to AE2) and desorbs at higher T (from AE2 to DE). The remaining observables confirm the picture sketched so far. The center-of-mass distance to the surface $\langle z_{\mathrm{cm}} \rangle$ gives a clear signal of the adsorption transition, whose location is well described by $T_{\mathrm{ads}} \propto \epsilon_s$. Since at higher T the stronger thermal fluctuations are more likely to overcome the surface attraction, this is intuitive. The mean number of surface contacts supports the observed layering.

It is clear that in particular in the compact pseudo-phases the structural behavior of the studied small chains is affected by finite-size effects. However, especially at high temperatures, the pseudo-phase diagram constructed here corresponds quite well with a similar lattice study [8] with the advantage of not suffering from lattice artifacts.

4. The adsorption transition revisited microcanonically

We now concentrate on the adsorption transition and look at it from another perspective: the microcanonical one. This approach has already proven quite useful for first-order-like structural transitions such as molecular aggregation processes [16,17] and protein folding [18,19]. For more details on this work see Ref. [20].
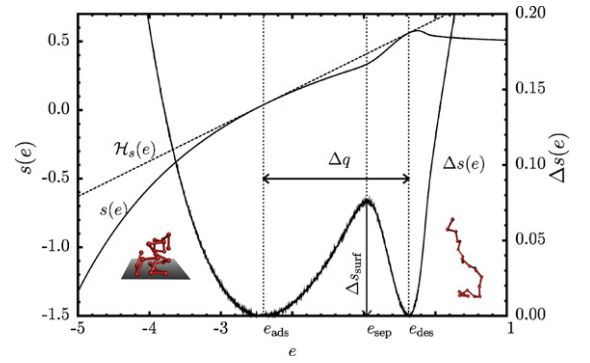

Fig. 4. Microcanonical entropy $s(e)$ (up to a constant) for a 20mer at $\epsilon_s = 5$, the Gibbs hull $\mathcal{H}_s(e)$, and the difference $\Delta s(e) = \mathcal{H}_s(e) - s(e)$ versus energy per monomer e. The local maximum of $\Delta s(e)$, called surface entropy Δs_{surf}, defines the energy of phase separation. The latent heat Δq is defined as the energy being necessary to cross the transition region at the transition temperature T_{ads}.

The central quantity is the density of states $g(E)$ or the microcanonical entropy defined as $S(E) \equiv \ln g(E)$. Here, we normalize everything by the number of monomers and use

$$s(e) = N^{-1} \ln g(e), \qquad (3)$$

with $e = E/N$. In contrast to canonical (NVT) statistics, where T is an externally fixed control parameter, in the microcanonical (NVE) ensemble it is *derived* from the entropy, $T(e) = [\partial s(e)/\partial e]_{N,V}^{-1}$. There are cases for finite systems, where $s(e)$ is a convex function in a transition regime. A consequence is that with *increasing* system energy the temperature *decreases*. This is true as long as the surface-to-volume ratio is large enough to suppress a concave increase of $s(e)$. In such a case, the energetic separation of the two distinct phases is sufficiently large to establish a kinetic barrier. This regards all first-order phase transitions and two-state systems, but also transitions, where phase coexistence is completely absent in the thermodynamic limit, but not for the finite system. The latter is the case here: The adsorption transition of flexible polymers to an attractive substrate is known to be continuous in the thermodynamic limit. However, as we will show here, the adsorption of finite non-grafted polymers exhibits signals of a first-order transition which vanish in the thermodynamic limit.

Exemplified for a 20mer and $\epsilon_s = 5$, we have plotted in Fig. 4 the microcanonical entropy $s(e)$. It shows the characteristic features of a transition with phase coexistence in a small system. For energies right below e_{ads}, the system is in the adsorbed phase AE2 (cf. Fig. 1), for $e_{\mathrm{ads}} < e < e_{\mathrm{des}}$, the system is in the transition region, where $s(e)$ is convex. One can construct the Gibbs hull

$$\mathcal{H}_s(e) = s(e_{\mathrm{ads}}) + e(\partial s/\partial e)_{e=e_{\mathrm{ads}}} \qquad (4)$$

as the tangent that touches $s(e_{\mathrm{ads}})$ and $s(e_{\mathrm{des}})$, whose inverse slope $T_{\mathrm{ads}} = (\partial \mathcal{H}_s/\partial e)^{-1}$ is the microcanonical *definition* of the adsorption temperature. However, the transition rather spans a region of temperatures like the fluctuation maxima do in the canonical ensemble. Hence, this adsorption temperature definition is not the only one possible. A unique transition point only exists in the thermodynamic limit. Nevertheless, not only for systems, where the thermodynamic limit is unreachable [21] in principle such as for proteins, it is worthwhile to understand the behavior of such a quantity. For a further analysis, we also use the surface (or interfacial) entropy, representing the entropic barrier of the transition, $\Delta s_{\mathrm{surf}} = \max\{\Delta s(e) = \mathcal{H}_s(e) - s(e) \mid e_{\mathrm{ads}} \leqslant e \leqslant e_{\mathrm{des}}\}$ and the latent heat, $\Delta q = e_{\mathrm{des}} - e_{\mathrm{ads}}$. Before we show for the adsorption transition that Δq decreases with N, we first investigate the origin of the phase separation for finite chains.
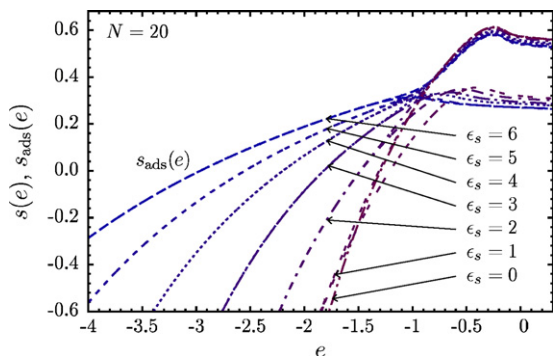
Fig. 5. Microcanonical entropy $s(e)$ and its fraction for adsorbed conformations $s_{ads}(e)$ at various surface attraction strengths $\epsilon_s = 0, 1, \ldots, 6$ for a 20mer [for all ϵ_s, the fraction for desorbed structures, $s_{des}(e)$, resembles $s(e)$ for $\epsilon_s = 0$].

4.1. Dependence on the surface attraction strength

In Fig. 5, $s(e)$ is shown for a 20mer and different ϵ_s, where here also $\epsilon_s = 6$ has been included. Since the high-energy regime is dominated by desorbed conformations, $s(e)$ is hardly affected by ϵ_s here, while the low-energy tail increases significantly with ϵ_s. Thus, one can split the density of states into contributions of desorbed and adsorbed conformations, $g_{des}(e)$ and $g_{ads}(e)$, respectively, such that $g(e) = g_{des}(e) + g_{ads}(e)$ and $s_{des,ads}(e) = N^{-1} \ln g_{des,ads}(e)$. We consider the polymer to be adsorbed if $E_{surf} < -0.1\epsilon_s N$. This choice includes all polymers that are reasonably strongly adsorbed in terms of energy and works for all ϵ_s. Moreover, qualitative features do not depend sensitively on the choice and this devision is only employed to get a qualitative picture, not to extract Δq or Δs_{surf}. Since both, $s_{ads}(e)$ and $s_{des}(e)$, are concave in the whole energy range of the transition, the convex entropic monotony can only occur in the region, where adsorbed and desorbed conformations have similar entropic weight.

Performing the Gibbs construction as in Fig. 4 to extract $\Delta s(e)$, one sees [20] that for $\epsilon_s \gtrsim 2$ the transition appears to be first-order like ($\Delta q = e_{des} - e_{ads} > 0$) for a finite, non-grafted chain. For $\epsilon_s \lesssim 2$, the Gibbs construction is no longer meaningful in absence of a convex regime in $s(e)$, indicating a second-order phase transitions ($\Delta q = 0$). Referring to the phase diagram in Fig. 1, the adsorption transition thus seems to become first-order-like at that point, where it falls together with the Θ-transition ($\epsilon_s \approx 1.8$, $T \approx 1.3$). This is also signaled by the saddle point of the corresponding $T^{-1}(e)$ curve. For larger ϵ_s, phase coexistence gets apparent between DE and AE2. Here, Δs_{surf} and Δq increase with ϵ_s and trivially diverge for $\epsilon_s \to \infty$. Also the first-order-like features of $T^{-1}(e)$ increase and the adsorption temperatures T_{ads} depend roughly linearly on ϵ_s, as was already suggested by the canonical data.

4.2. Chain-length dependence

Since the adsorption transition is expected to be of second order in the thermodynamic limit [5], first-order signatures found for the finite system between DE and AE2 must disappear for $N \to \infty$. Indeed, our data for N up to $N = 150$ support a power-law scaling of the latent heat, $\Delta q \sim N^{-\kappa_q}$, with $\kappa_q \approx 0.35$–0.40, which clearly suggests $\lim_{N \to \infty} \Delta q = 0$, confirming this expectation.

4.3. Variation of the box size

After noticing that there is a considerable influence of the simulation box size on $s(e)$, we also investigated this effect. To this end, simulations with fixed $\epsilon_s = 5$ and chain length $N = 20$ were performed for different $L_z = 20, 30, \ldots, 150$. Because the number

of adsorbed conformations cannot depend on L_z, the unknown additive constants to $s(e)$, $s_{ads}(e)$, and $s_{des}(e)$ were chosen such that $s_{ads}(e)$ coincides for all L_z. With this choice, $s_{des}(e)$ increases with the logarithm of L_z, like it should be the case for the *translational* entropy. Consequently, both, the surface entropy Δs_{surf} and the latent heat Δq increase with L_z. Note, that in the case of a grafted polymer, effectively corresponding to a small L_z, we did not observe any convex intruder in the microcanonical entropy.

5. Summary

In this work, we have used two approaches to describe the behavior of a single homopolymer near an attractive substrate.

First, in analyses of canonical expectation values of several energetic and structural quantities and their thermal fluctuations for a chain with 20 monomers, conformational phases and phase boundaries in the pseudo-phase diagram versus temperature and surface attraction strength were identified. Our chosen simulational method was the multicanonical Monte Carlo technique. Although the computational expense to accurately explore such a broad parameter range restricted us to rather short chains, for the majority of pseudo-phases, in particular those that are assumed to be relevant in the thermodynamic limit, we find a nice qualitative coincidence with similar lattice studies. Then, we complemented the picture by focusing on the adsorption transition microcanonically. For short polymers, the microcanonical entropy revealed that at the adsorption transition adsorbed and desorbed conformations coexist, corresponding to a first-order character of this transition for short polymers. We have studied how the character of this transition depends on surface attraction strength, chain length, and concentration.

Altogether, our study has shown the usefulness of a combined approach of the microcanonical and canonical ensemble in understanding the conformational behavior of finite systems.

References

[1] B. Alberts, D. Bray, A. Johnson, J. Lewis, M. Raff, K. Roberts, P. Walter, Essential Cell Biology, Garland Publishing, Inc., New York, 1998.
[2] M. Breidenich, R.R. Netz, R. Lipowsky, Adsorption of polymers anchored to membranes, Eur. Phys. J. E 5 (2001) 403–414.
[3] M. Sarikaya, C. Tamerler, A.K.-Y. Jen, K. Schulten, F. Baneyx, Molecular biomimetics: nanotechnology through biology, Nature Mater. 2 (2003) 577–585.
[4] M. Bachmann, K. Goede, A.G. Beck-Sickinger, M. Grundmann, A. Irbäck, W. Janke, Microscopic mechanism of specific peptide adhesion to semiconductor substrates, Angew. Chem. Int. Ed. 49 (2010) 9530–9533.
[5] E. Eisenriegler, Polymers Near Surfaces: Conformation Properties and Relation to Critical Phenomena, World Scientific, Singapore, New Jersey, 1993.
[6] J. Krawczyk, A.L. Owczarek, T. Prellberg, A. Rechnitzer, Layering transitions for adsorbing polymers in poor solvents, Europhys. Lett. 70 (2005) 726–732.
[7] K. Binder, J. Baschnagel, M. Müller, W. Paul, F. Rampf, Simulation of phase transitions of single polymer chains: recent advances, Macromol. Symp. 237 (2006) 128–138.
[8] M. Bachmann, W. Janke, Substrate adhesion of a nongrafted flexible polymer in a cavity, Phys. Rev. E 73 (2006) 041802 (1-8).
[9] M. Möddel, M. Bachmann, W. Janke, Conformational mechanics of polymer adsorption transitions at attractive substrates, J. Phys. Chem. B 113 (2009) 3314–3323.

[10] B.A. Berg, T. Neuhaus, Multicanonical algorithms for first order phase transitions, Phys. Lett. B 267 (1991) 249–253;
B.A. Berg, T. Neuhaus, Multicanonical ensemble: a new approach to simulate first-order phase transitions, Phys. Rev. Lett. 68 (1992) 9–12.

[11] F.H. Stillinger, T. Head-Gordon, C.L. Hirshfeld, Toy model for protein folding, Phys. Rev. E 48 (1993) 1469–1477;
F.H. Stillinger, T. Head-Gordon, Collective aspects of protein folding illustrated by a toy model, Phys. Rev. E 52 (1995) 2872–2877.

[12] S. Schnabel, M. Bachmann, W. Janke, Two-state folding, folding through intermediates, and metastability in a minimalistic hydrophobic-polar model for proteins, Phys. Rev. Lett. 98 (2007) 048103 (1-4);
S. Schnabel, M. Bachmann, W. Janke, Identification of characteristic protein folding channels in a coarse-grained hydrophobic-polar peptide model, J. Chem. Phys. 126 (2007) 105102 (1-6).

[13] W.A. Steele, The physical interaction of gases with crystalline solids: I. Gas—solid energies and properties of isolated adsorbed atoms, Surf. Sci. 36 (1973) 317–352.

[14] W. Janke, Multicanonical Monte Carlo simulations, Physica A 254 (1998) 164–178;
B.A. Berg, Introduction to multicanonical Monte Carlo simulations, Fields Inst. Commun. 26 (2000) 1–24.

[15] Y. Singh, D. Giri, S. Kumar, Crossover of a polymer chain from bulk to surface states, J. Phys. A 34 (2001) L67–L74.

[16] C. Junghans, M. Bachmann, W. Janke, Microcanonical analyses of peptide aggregation processes, Phys. Rev. Lett. 97 (2006) 218103 (1-4);
C. Junghans, M. Bachmann, W. Janke, Thermodynamics of peptide aggregation processes: an analysis from perspectives of three statistical ensembles, J. Chem. Phys. 128 (2008) 085103 (1-9).

[17] C. Junghans, M. Bachmann, W. Janke, Statistical mechanics of aggregation and crystallization for semiflexible polymers, Europhys. Lett. 87 (2009) 40002 (1-5).

[18] T. Chen, X. Lin, Y. Liu, H. Liang, Microcanonical analysis of association of hydrophobic segments in a heteropolymer, Phys. Rev. E 76 (2007) 046110 (1-4).

[19] J. Hernández-Rojas, J.M. Gomez Llorente, Microcanonical versus canonical analysis of protein folding, Phys. Rev. Lett. 100 (2008) 258104 (1-4).

[20] M. Möddel, W. Janke, M. Bachmann, Systematic microcanonical analyses of polymer adsorption transitions, Phys. Chem. Chem. Phys. 12 (2010) 11548–11554.

[21] M. Bachmann, W. Janke, Multicanonical chain-growth algorithm, Phys. Rev. Lett. 91 (2003) 208105 (1-4);
M. Bachmann, W. Janke, Thermodynamics of lattice heteropolymers, J. Chem. Phys. 120 (2004) 6779–6791.